Novel Thiophene–Phenylene–Thiophene Fused Bislactam-Based Donor–Acceptor Type Conjugate Polymers: Synthesis by Direct Arylation and Properties

ARTICLE *in* MACROMOLECULES · NOVEMBER 2013

Impact Factor: 5.8 · DOI: 10.1021/ma4018907

Macromolecules

Article

pubs.acs.org/Macromolecules

Novel Thiophene−Phenylene−Thiophene Fused Bislactam-Based Donor−Acceptor Type Conjugate Polymers: Synthesis by Direct Arylation and Properties

Mithrabinda K. Poduval,[†] Paula Mayorga Burrezo,[‡] Juan Casado,[‡] J. Teodomiro López Navarrete,*[,‡] Rocío Ponce Ortiz,*[,‡] and Tae-Hyun Kim*[,†]

[†]Organic Material Synthesis Laboratory, Department of Chemistry, Incheon National University, Songdo-dong 12-1, Yeonsu-gu, Incheon 406-840, Korea

[‡]Department of Physical Chemistry, University of Málaga, 29071 Málaga, Spain

Supporting Information

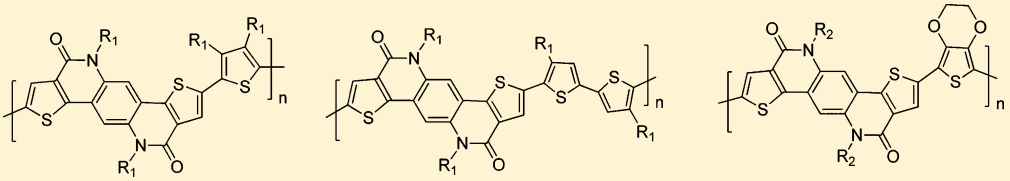

P1 ($R_1 = C_{12}H_{25}$) **P2** ($R_1 = C_{12}H_{25}$) **P3** ($R_2 = CH_2CH(C_8H_{17})(C_6H_{13})$)

ABSTRACT: Three new donor−acceptor copolymers based on thiophene−phenylene−thiophene fused bislactam and various donors (3,4-dodecylthiophene, 4,4′-didodecyl-2,2′-bithiophene, and ethylenedioxythiophene) were synthesized, characterized, and used in field-effect transistors. Polycondensation was performed using nonactivated thiophene derivatives by employing palladium-catalyzed direct arylation under phosphine-free conditions. This method is superior to traditional cross-coupling polymerization because it requires fewer synthetic operations and does not employ toxic organometallic intermediates. Regioselective polymers can also be generated by using β-substituted thiophene derivatives. The studied polymers were tested in a bottom gate top contact thin film transistor (OTFT) architecture. The best electronic performance was shown by polymer **P3**, with enhanced π-conjugation due to the appearance of intramolecular attractive interactions.

1. INTRODUCTION

Organic conjugated polymers can be used to fabricate optoelectronic devices, including unipolar/complementary circuits, light-emitting diodes, field effect transistors, photovoltaics, and sensors.[1−16] As these technologies become commercialized, larger quantities of the active compounds will be needed, making the efficient synthesis of these compounds necessary. Among the most promising families of conjugated polymers in this field are those based on homo- and copolymers of heterocyclics such as poly(thiophene)s;[17−20] fused (hetero)-arenes such as poly(thienothiophene)s,[21,22] poly(carbazole)-s,[23,24] poly(benzodithiophene)s; and rylenes[25−27] such as poly[naphthalene bis(dicarboxiimide)]s. These materials are usually synthesized by traditional metal-catalyzed cross-coupling reactions, including the Suzuki, Stille, Negishi, and Kumada reactions. Despite their great versatility, these methods have drawbacks, including the need for numerous synthetic steps to prepare monomers and the instability of the organometallic reagents. In addition, stoichiometric amounts of toxic byproducts are produced. One alternative to traditional cross-coupling is direct arylation, in which the organometallic component is replaced by a simple unfunctionalized (hetero)arenes and coupled through C−H bond cleavage.[15,28−32] Although this method has been used to synthesize small molecules, it has seldom been used to synthesize organic conjugated polymers, with few examples published in the field of polymer synthesis using direct arylation-based polycondensation.[33−36] Another challenge for direct arylation is the need for high regioselectivity, as several C−H bonds exhibit comparable dissociation energies. Although several (hetero)arenes show preferential reactive positions, and this was utilized in the highly regioselective metal-catalyzed direct funtionalization between electron-rich and electron-poor (hetero)arenes, reactions of electronically unbiased (hetero)arenes are often nonselective, causing undesired mixtures of regioisomers.

Conjugated polymers with donor−acceptor (D−A) architectures are of particular interest because their electronic and optoelectronic properties could be efficiently tuned by intramolecular charge transfer (ICT), leading to low band gap semiconductors with relatively high charge carrier mobilities.[37−42] Hybridization of the HOMO on the donor moiety and the LUMO on the acceptor moiety provides a means to tune

Received: September 12, 2013
Revised: November 16, 2013

   dx.doi.org/10.1021/ma4018907 | Macromolecules XXXX, XXX, XXX−XXX

Chart 1. Molecular Structures of TPTBL-Based D−A Copolymers

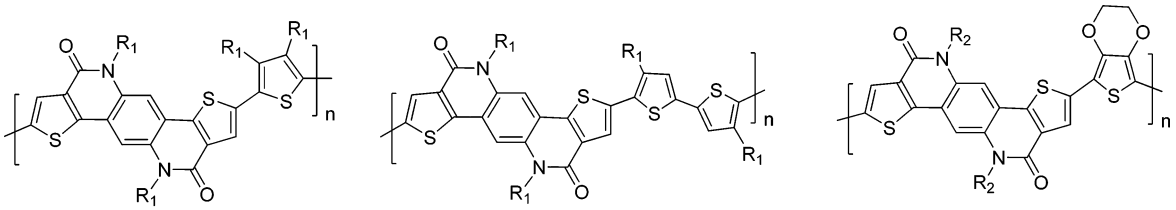

P1 ($R_1 = C_{12}H_{25}$) **P2** ($R_1 = C_{12}H_{25}$) **P3** ($R_2 = CH_2CH(C_8H_{17})(C_6H_{13})$)

the electronic and optoelectronic properties for device applications. Thiophene and its derivatives are among the most common donor moieties, and several conjugated polymers based on thiophene−acceptor or thiophene−acceptor−thiophene polymer systems have shown high FET mobilities.[43−48] Mobility, however, was reported to be further controlled by the acceptor strength and/or the manipulation of the acceptor structure. For example, D−A conjugated copolymers containing strong electron acceptors bearing imide or lactam groups, such as naphthalenebisimide and diketopyrrolopyrrole, have recently been found to exhibit strong intramolecular charge transfer, leading to excellent intramolecular planarity and good electron transport properties.[49−52] The exploration of a new acceptor is thus a compelling subject in this chemistry.

As a new entry into this class of materials, we report herein three new conjugated polymers based on the thiophene−phenylene−thiophene fused bislactam (TPTBL) as a strong electron acceptor. Polymerization was carried out using Pd-catalyzed direct arylation between brominated TPTBL and, as coupling donor monomers, 3,4-dodecylthiophene (DT), 4,4′-didodecyl-2,2′-bithiophene (DBT), and ethylenedioxythiophene (EDOT). Since substituted thiophene derivatives are used as nonactivated coupling components, highly regioselective direct arylation with brominated TPTBL was expected.

The molecular structures of the new TPTBL-based D−A copolymers (**P1**, **P2**, and **P3**) are shown in Chart 1. The morphology of the solution-cast films of the three D−A copolymers was investigated by X-ray diffraction. The electronic structure (HOMO/LUMO levels) of the new polymers was estimated by cyclic voltammetry on thin films while their molecular structures were analyzed by Raman vibrational spectroscopy aided by DFT theoretical calculations. The field effect carrier mobility was obtained from the bottom gate top contact thin film transistor (TFT) devices and correlated with the polymer structure.

2. EXPERIMENTAL SECTION

2.1. Materials and Synthetic Procedures. *Materials.* All commercially available reagents were used without further purification.

*Synthetic Procedure. N,N′-(1,4-Phenylene)bis(2-bromothiophene-3-carboxamide), **3**.* To a solution of *p*-phenelynediamine (200 mg, 1.93 mmol) in NMP at −5 °C under a nitrogen atmosphere, 2-bromothiophene-3-carbonyl chloride (900 mg, 3.91 mmol) was added. The reaction mixture was stirred for 30 min at this temperature and was left to stir at rt for another 3 h. The white precipitate formed was then filtered and washed with acetone several times, collected, and dried under vacuum to give the compound **3** as a white powder (900 mg, 96%); mp 268−269 °C. ν_{max} (KBr)/cm^{-1} 3274, 2917, 1646, 1544, 1517, 1413, 1313, 1253, 1099, 993, and 815. *m*/*z* (FAB) 487 (6%), 391 (11%), 157 (64%), and 79 (100%) [Found (M + H)$^+$ 484.8622. $C_{16}H_{11}Br_2N_2O_2S_2$ requires *M*, 484.8629].

*N,N′-(1,4-Phenylene)bis(2-bromo-N-dodecylthiophene-3-carboxamide), **4**.* To a suspension of compound **3** (750 mg, 1.54 mmol) in DMF (7 mL) at rt under a nitrogen atmosphere, 60% of sodium hydride (250 mg, 7.71 mmol) was added. After a vigorous stirring for 10 min, 1-iodododecane (115 mg, 4.62 mmol) was added slowly, and the reaction mixture was left to stir for 5 h at this temperature. The mixture was then extracted with ethyl acetate (3 times), and the combined organic layers were washed with HCl (1 M, 20 mL), water, and brine. The organic layer was dried over $MgSO_4$, filtered, and concentrated by vacuum. The crude product was purified by recrystallization from ethyl acetate−hexane mixture (1:1) to give the compound **4** as white crystals (660 mg, 70%); mp 74−75 °C. R_f: 0.16 (5:1, Hex:EtOAc). ν_{max} (KBr)/cm^{-1} 2917, 2850, 1637, 1509, 1415, 1292, 1143, 850 and 703. ^{1}H NMR (400 MHz, $CDCl_3$, δ) 7.01 (2H, d, J = 5.5 Hz, 2 × *ArH*), 6.93 (4H, s, 4 × ArH), 6.59 (2H, d, J = 5.5 Hz, 2 × *ArH*), 3.84 (4H, t, J = 7.0 Hz, 2 × (NCH_2−)), 1.55 (4H, m, 2 × (CH_2)), 1.25 (36H, multiplet containing quintet, J = 6.3 Hz, 2 × (CH_2)$_9$) and 0.88 (6H, t, J = 6.3 Hz, 2 × CH_3). ^{13}C NMR (100 MHz, $CDCl_3$, δ) 164.79, 140.46, 137.61, 129.69, 127.40, 126.39, 111.89, 49.55, 31.89, 29.54, 29.30, 27.77, 26.78, 22.69, and 14.13. *m*/*z* (FAB) 823 (60%), 743 (10%), 633 (41%), and 191 (100%) [Found (M + H)$^+$ 821.2376. $C_{40}H_{59}Br_2N_2O_2S_2$ requires *M*, 821.2385].

*N,N′-(1,4-Phenylene)bis[2-bromo-N-(2-hexyldecane) thiophene-3-carboxamide], **4a**.* To a suspension of compound **3** (800 mg, 1.64 mmol) in DMF (10 mL) at rt under a nitrogen atmosphere, 60% of sodium hydride (395 mg, 16.45 mmol) was added. After a vigorous stirring for 10 min, 1-bromo-2-hexyldecane (105 mg, 3.62 mmol) was added slowly, and the reaction mixture was left to stir for 5 h at this temperature. The mixture was then extracted with ethyl acetate (3 times), and the combined organic layers were washed with HCl (1 M, 20 mL), water, and brine. The organic layer was dried over $MgSO_4$, filtered, and concentrated by vacuum. The crude product was purified by recrystallization from ethyl acetate−hexane mixture (1:1) to give compound **4a** as viscous oil (400 mg, 26%); R_f: 0.26 (5:1, Hex:EtOAc). ν_{max} (KBr)/cm^{-1} 2916, 2850, 1630, 1496, 1410, 1291, 1135, 859, and 701. ^{1}H NMR (400 MHz, $CDCl_3$, δ) 6.98 (2H, d, J = 5.5 Hz, 2 × *ArH*), 6.92 (4H, s, 4 × *ArH*), 6.53 (2H, d, J = 5.5 Hz, 2 × *ArH*), 3.81 (4H, ABq, J = 7.0 Hz, 2 × (NCH_2−)), 1.41 (4H, m, 2 × (CH_2)), 1.25 (44H, multiplet containing quintet, J = 5.7 Hz, 2 × (CH_2)$_{11}$) and 0.88 (12H, t, J = 5.7 Hz, 4 × CH_3). ^{13}C NMR (100 MHz, $CDCl_3$, δ) 164.22, 139.37, 136.94, 126.59, 126.27, 125.31, 110.70, 51.35, 44.51, 35.09, 30.93, 28.57, 28.37, 25.36, 21.69, and 13.12.

*Cyclization to the Thiophene−Phenylene−Thiophene-Based Fused Bislactam (TPTL) with a Dodecyl Substituent, **5**.* Compound **4** (450 mg, 0.546 mmol), $Pd(OAc)_2$ (12.25 mg, 0.054 mmol), and sodium acetate (134.5 mg, 1.64 mmol) were all taken in a Schlenk flask under a nitrogen atmosphere. To this flask anhydrous DMAc (4 mL) was added, and the reaction mixture was heated to 130 °C and left to stir for 12 h. The precipitate was then filtered through a short column of Celite using chloroform as eluant. The filtrate was collected and washed with water several times, and the combined organic layers were dried over magnesium sulfate and this was concentrated under reduced pressure. The crude product was purified by recrystallization from ethyl acetate−hexane mixture (1:1) to give compound **5** as yellow crystals (250 mg, 69%); mp 166−167 °C; R_f: 0.32 (5:1, Hex:EtOAc). ν_{max} (KBr)/cm^{-1} 2917, 2850, 1648, 1465, 1395, 1276, 1059, 846, and 725. ^{1}H NMR (400 MHz, $CDCl_3$, δ) 7.79 (2H, d, J = 5.5 Hz, 2 × *ArH*,), 7.75

dx.doi.org/10.1021/ma4018907 | *Macromolecules* XXXX, XXX, XXX−XXX

(2H s, 2 × *ArH*), 7.45 (2H, d, *J* = 5.5 Hz, 2 × *ArH*), 4.45 (4H, t, *J* = 7.2 Hz, 2 × (*N*−CH_2)), 1.86 (4H, quintet, *J* = 7.2 Hz, 2 × (−CH_2)−), 1.44 (4H, quintet, *J* = 7.2 Hz, 2 × (−CH_2)−), 1.27 (32H, multiplet containing quintet, *J* = 6.3 Hz, 2 × $(CH_2)_8$), and 0.88 (6H, t, *J* = 6.3 Hz, 2 × CH_3). ^{13}C NMR (100 MHz, $CDCl_3$, δ) 158.13, 144.26, 132.04, 131.87, 127.22, 125.61, 119.54, 109.68, 42.41, 31.93, 29.67, 29.38, 27.46, 27.03, 22.70, and 14.14; *m*/*z* (FAB) 661 (62%), 493 (8%), 307 (20%), 154 (100%) [Found (M + H)$^+$ 661.3870. $C_{40}H_{57}N_2O_2S_2$ requires *M*, 661.3861].

Cyclization to the Thiophene−Phenylene−Thiophene-Based Fused Bislactam (TPTL) with a 2-Hexyl-1-decyl Substituent, ***5a.*** This was prepared essentially in the same manner as that of the TPTL **5**. Compound **5a** was obtained as yellow crystals (220 mg, 65%); mp 120−122 °C; R_f: 0.50 (5:1, Hex:EtOAc). ν_{max} (KBr)/cm^{-1} 2915, 2850, 1650, 1470, 1396, 1273, 1059, 840, and 724. ^{1}H NMR (400 MHz, $CDCl_3$, δ) 7.75 (2H, d, *J* = 5.5 Hz, 2 × *ArH*), 7.63 (2H, s, 2 × *ArH*), 7.42 (2H, d, *J* = 5.5 Hz, 2 × *ArH*), 4.31 (4H, m, ABq, *J* = 6.3 Hz, 2 × (*N*−CH_2)), 1.96 (2H, m, 2 × (*CH*−)), 1.43 (4H, m, 2 × (CH_2)), 1.26 (48H, m, 2 × (−CH_2−)$_{12}$), and 0.88 (12H, t, *J* = 6.3 Hz, 4 × (CH_3)). ^{13}C NMR (100 MHz, $CDCl_3$, δ) 158.55, 144.17, 132.06, 131.73, 127.38, 125.41, 119.18, 110.01, 45.95, 36.92, 31.81, 30.06, 29.56, 29.28, 27.04, 22.67, and 14.08.

Brominated TPTL with a Dodecyl Substituent, ***6.*** To a solution of compound **5** (100 mg, 0.151 mmol) in chloroform (1 mL), bromine (1 mL, 1 molar in acetic acid) was added dropwise at rt. The reaction mixture was then stirred for 3 h at rt under a nitrogen atmosphere. After completion of the reaction, which was confirmed by TLC, chloroform was evaporated, and the yellow solid was washed several times with water. The powder was collected and recrystallized from a mixture of ethyl acetate and chloroform (5:1) to give the brominated TPTL ***6*** as a yellow crystal (123 mg, 100%); mp 273−274 °C; R_f: 0.64 (5:1, Hex:EtOAc). ν_{max} (KBr)/cm^{-1} 2917, 2850, 1641, 1467, 1390, 1238, 1060, and 844. ^{1}H NMR (400 MHz, $CDCl_3$, δ): 7.72 (2H, s, 2 × *ArH*), 7.52 (2H, s, 2 × *ArH*), 4.37 (4H, t, *J* = 7.2 Hz, 2 × (*N*−CH_2)), 1.80 (4H, quintet, *J* = 7.24 Hz, 2 × (−CH_2)), 1.51 (4H, m, 2 × −(CH_2−)), 1.49 (4H, m, 2 × (CH_2−)), 1.28 (28H, multiplet containing quintet, *J* = 6.3 Hz, 2 × $(CH_2)_7$), and 0.88 (6H, t, *J* = 6.3 Hz, 2 × (CH_3)). ^{13}C NMR (100 MHz, $CDCl_3$, δ) 156.71, 145.15, 132.29, 132.07, 129.65, 118.81, 114.22, 109.44, 42.51, 31.92, 29.58, 29.23, 26.97, 22.69, and 14.14. *m*/*z* (FAB) 818 (8%), 396 (100%), and 368 (47%) [Found M$^+$ 816.1999. $C_{40}H_{54}Br_2N_2O_2S_2$ requires *M*, 816.1993].

Brominated TPTL with a 2-Hexyl-1-decyl Substituent, ***6a.*** This was prepared essentially in the same manner as that of the brominated-TPTL **6**. Compound **6a** was obtained as yellow crystals (90 mg, 100%); mp 273−274 °C; R_f: 0.43 (10:1, Hex:EtOAc). ν_{max} (KBr)/cm^{-1} 2917, 2850, 1641, 1467, 1390, 1238, 1060, and 844. ^{1}H NMR (400 MHz, $CDCl_3$, δ) 7.73 (2H, s, 2 × *ArH*), 7.57 (2H, s, 2 × *ArH*), 4.36 (4H, ABq, *J* = 6.3 Hz, 2 × (*N*−CH_2)), 1.95 (2H, quintet, *J* = 7.2 Hz, 2 × (−CH_2−)), 1.44 (4H, m, 2 × (CH_2−)), 1.34 (4H, m, 2 × (CH_2−)), 1.28 (48H, m, 2 × $(CH_2)_{12}$), and 0.88 (12H, t, *J* = 6.3 Hz, 4 × (−CH_3)). ^{13}C NMR (100 MHz, $CDCl_3$, δ) 157.35, 145.24, 132.23, 129.83, 119.33, 118.64, 109.99, 46.17, 36.98, 31.89, 29.61, 29.30, 27.11, 22.65, and 14.13.

Poly[(thiophene−phenylene−thiophene)-alt-(3,4-didodecylthiophene)], ***P1.*** The brominated compound **6** (125 mg, 0.152 mmol), 3,4-didodecylthiophene (67 mg, 0.152 mmol), $Pd(OAc)_2$ (3.41 mg, 0.015 mmol), and sodium acetate (49.92 mg, 0.608 mmol) were all transferred in a Schlenk flask under a nitrogen atmosphere. The anhydrous DMAc (4 mL) was then added, and the whole reaction mixture was left to stir at 130 °C for 12 h. The resultant mixture was poured into 100 mL of methanol. The red precipitate was filtered and further purified by Soxhlet extraction using methanol, acetone, and hexane to remove any remaining salts or oligomers to give the desired polymer **P1** as red powder (90 mg, 53%). GPC ($CHCl_3$, RI) Da, M_n = 7.6 × 10^3, M_w = 14.8 × 10^3. TGA%/°C 90/420, 80/451. ν_{max} (KBr)/cm^{-1} 2917, 2850, 1640, 1560, 1457, 1457, 1214, 1079, and 750. ^{1}H NMR (400 MHz, $CDCl_3$, δ) 7.70 (2H, broad signal, 2 × *ArH*), 7.66 (2H, broad signal, 2 × *ArH*), 4.44 (4H, broad signal, 2 × (*N*−CH_2)), 2.76 (4H, broad signal, 2 × (−CH_2)), 2.53 (4H, broad signal, 2 × (−CH_2)), 1.85 (4H, broad signal, 2 × (−CH_2)), 1.10 (36H, broad signal, 2 × (−CH_2)$_9$), and 0.84 (12H, broad signal, 4 × (CH_3)).

Poly[(thiophene−phenylene−thiophene)-alt-(5,5′-dibromo-4,4′-didodecyl-2,2′-bithiophene)], ***P2.*** This was prepared essentially in the same manner as that of **P1** except the use of 4,4′-didodecyl-2,2′-bithiophene (30.62 mg, 0.06 mmol) instead of 3,4-didodecylthiophene. Polymer **P2** was obtained as dark red powder (50 mg, 70%). GPC ($CHCl_3$, RI) Da, M_n = 8.9 × 10^3, M_w = 24.0 × 10^3. TGA%/°C 90/361, 80/454. ν_{max} (KBr)/cm^{-1} 2921, 2850, 1635, 1459, 1375, 1214, 1052, and 842. ^{1}H NMR (400 MHz, $CDCl_3$, δ) 7.71 (2H, broad signal, 2 × *ArH*), 7.64 (2H, broad signal, 2 × *ArH*), 7.00 (2H, broad signal, 2 × *ArH*), 4.45 (4H, broad signal, 2 × (NCH_2)−), 2.83 (4H, broad signal, 2 × (−CH_2)), 2.54 (4H, broad signal, 2 × (−CH_2)), 1.85 (4H, broad signal, 2 × (−CH_2)), 1.25 (36H, broad signal, 2 × (−CH_2)$_9$), and 0.86 (12H, broad signal, 4 × (−CH_3)).

Poly[(thiophene−phenylene−thiophene)-alt-(ethylenedioxythiophene)], ***P3.*** This was prepared essentially in the same manner as that of **P1** except the use of ethylenedioxythiophene (15.65 mg, 0.110 mmol) instead of 3,4-didodecylthiophene. Polymer **P3** was obtained as pink powder (65.0 mg, 68%). GPC ($CHCl_3$, RI) Da, M_n = 8.2 × 10^3, M_w = 18.8 × 10^3. TGA%/°C 90/257, 80/316. ν_{max} (KBr)/cm^{-1} 2919, 2850, 1637, 1479, 1396, 1257, 1076, 1014, and 803. ^{1}H NMR (400 MHz, $CDCl_3$, δ) 7.60 (2H, s, 2 × *ArH*), 7.44 (2H, s, 2 × *ArH*), 4.41 (8H, broad signal, 2 × (NCH_2), and (*O*−CH_2−CH_2−*O*)), 1.80 (2H, broad signal, 2 × (−*CH*−)), 1.25 (48H, broad signal, 2 × (−CH_2)$_{12}$), and 0.84 (6H, broad signal, 2 × (−CH_3)).

Methods. ^{1}H NMR spectra were obtained on an Agilent 400-MR (400 MHz) instrument using $CDCl_3$ as a reference or internal deuterium lock. ^{13}C NMR spectra were recorded on a Bruker Advance-300 (75.4 MHz) instrument and Agilent 400-MR (100 MHz) instrument using internal deuterium lock and proton decoupling.

Mass spectra were obtained on a JEOL JMS-AX505WA instrument.

FT-IR spectra of the materials were recorded as KBr pellets using Nicolet MAGNA 560-FTIR spectrometer in the range of 4000−400 cm^{-1}.

Molar masses were determined by gel permeation chromatography (GPC) using two PL Gel 30 cm × 5 μm mixed C columns at 40 °C running in $CHCl_3$ and calibrated against polystyrene (M_n = 600−10^6 g/mol) standards using a Knauer refractive index detector.

Thermal stability of the polymer was analyzed by the thermogravimetric analysis measurements on a Shimadzu TGA-2950 instrument at a heating rate of 10 °C min^{-1} in a nitrogen flow. The glass transition temperature (T_g) was measured using a PerkinElmer Pyris-1 DSC from 20 to 260 °C with a scan rate of 10 °C min^{-1} under nitrogen.

FT-Raman spectra with 1064 nm excitation were recorded using a FT Raman accessory kit (FRA/106-S) of a Bruker Equinox 55 FT-IR interferometer and a continuous-wave Nd:YAG laser. A germanium detector operating at liquid-nitrogen temperature was used and the Raman scattering radiation was collected in a backscattering configuration with a 4 cm^{-1} spectral resolution. An average of 1000 scans was used in the reported spectra.

UV−vis absorption spectra of **P1**−**P3** dichloromethane solutions were recorded on an Agilent 8453 instrument equipped with a diode array detection system. Emission and excitation spectra were measured using a spectrofluorometer from Edinburgh Analytical Instrument (FLS920P) equipped with a pulsed xenon flash lamp, Xe900, of 400 mW. The transient absorption spectra were measured with an spectrometer from Luzchem (FLP-111) which includes a ceramic xenon light source of 300 W, 125 mm monochromator, and Tektronix digitizer TDS-3000 series with 300 MHz bandwidth. A Nd:YAG Lotis TII LS-2132 UTF laser working at 355 nm was employed for excitation.

Cyclic voltammetries were recorded for the polymeric thin films in a 0.1 M solution of tetrabutylammonium hexafluorophosphate in acetonitrile under a nitrogen flow and at a scan rate of 100 mV/s and using a BASi C3 cell stand. Platinum electrodes were used as both the working electrode and the counter electrode, and an Ag wire was used as the pseudoreference electrode. The ferrocene/ferrocinium (Fc/Fc^+) couple was used as internal reference ($E(Fc/Fc^+)$ in acetonitrile vs SCE = 0.391 V).

Density functional calculations were performed using the B3LYP functional[53] and 6-31G** basis set[54] as implemented in Gaussian 09.[55]

dx.doi.org/10.1021/ma4018907 | *Macromolecules* XXXX, XXX, XXX−XXX

Scheme 1. Synthesis of the Thiophene−Phenylene−Thiophene Fused Bislactams 5 and Their Brominated Forms 6

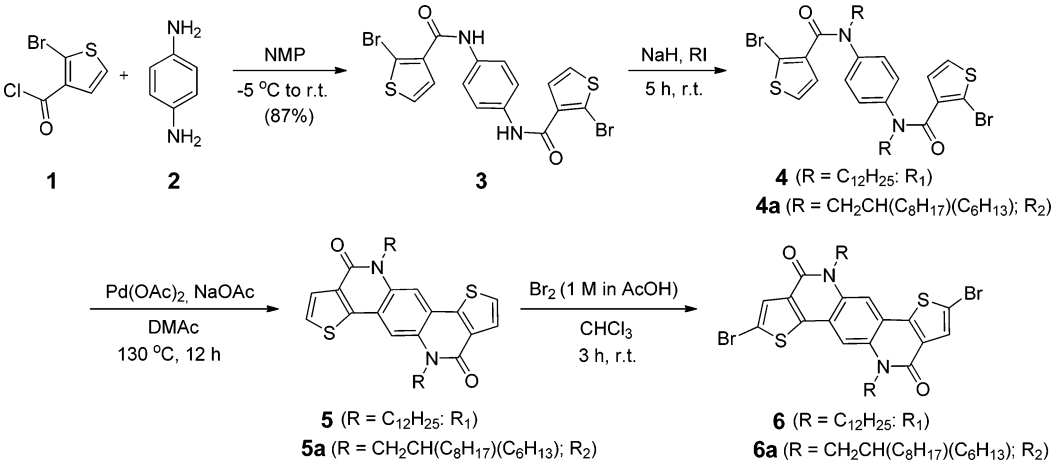

For thin film characterization, AFM images were recorded in a tapping mode on an atomic force microscope diMultiModeV Veeco Instruments-Nanoscope V, while the X-ray diffraction patterns were recorded using a Philips XPERT-PRO MRD diffractometer by employing a scanning range (2θ) from 1° to 10° with a Cu Kα_1 X-ray (λ = 1.540 598 Å).

Bottom-gate top-contact OTFTs were fabricated to investigate the charge transport properties of the **P1**−**P3** polymers. The semiconductor layers were deposited by spin-coating a 10 mg/mL polymer solution in chloroform under ambient conditions on hexamethyldisilazane (HMDS) and octadecyltrichlorosilane (OTS)-treated p-doped Si wafers with 300 nm thermally grown SiO_2 dielectric layers. The capacitance of the 300 nm SiO_2 gate insulator was 12 nF cm^{-2}. Prior to semiconductor deposition, the wafers were solvent cleaned by immersing them twice for 30 s each in EtOH with sonication, drying with a stream of N_2, and treating with UV-ozone for 10 min. The cleaned silicon wafers were treated with hexamethyldisilazane by exposing them to HMDS vapor at room temperature in a closed air-free container under argon and were treated with octadecyltrichlorosilane by inmersion in a 3.0 mM humidity-exposed OTS−hexane solution for 1 h, as previously described.[56] Following OTS deposition, the substrates were sonicated with hexane, acetone, and ethanol and dried with a N_2 stream. After semiconductor deposition, the films were annealed under vacuum at selected temperatures and iniatially analyzed by XRD and AFM techniques. OFET devices were completed by gold electrodes vapor deposition through a shadow mask to define devices with various channel lengths and channel widths. Devices were characterized under ambient conditions in an EB-4 Everbeing probe station with a 4200-SCS/C Keithley semiconductor characterization system.

3. RESULTS AND DISCUSSION

3.1. Synthesis and Characterization. The synthesis of the thiophene−phenylene−thiophene-based fused bislactam (TPTBL) acceptor is outlined in Scheme 1. The reaction of 2-bromothiophene acid chloride (**1**) with *p*-phenylenediamine (**2**) to produce bisamide **3**, followed by N-alkylation using NaH and dodecyl iodide or 2-hexyl-1-decyl iodide, yielded the precursor (**4** or **4a**) of the lactam acceptor. The alkyl substituents were introduced as solubilizing groups for the fused lactam, with the 2-hexyl-1-decyl group expected to provide greater solubility than the dodecyl group. Intramolecular cyclization by Pd-catalyzed direct arylation between 2-bromothiophene and amidobenzene produced the desired thiophene−phenylene−thiophene fused bislactams (TPTBL) **5** and **5a** as new acceptors. These reactions, performed in the absence of phosphine ligand and pivalic acid, the common additives for direct arylation, resulted in fairly good yields of **5** (69%) and **5a** (65%). Changes in color from white to yellow were observed after cyclization, with cyclization further confirmed by comparative ^{1}H NMR spectroscopic analysis, in which the two phenyl peaks next to the nitrogen atom were shifted downfield (6.93 to 7.75 ppm) and their integral was reduced by half.

Because of the strong electron-withdrawing nature of the lactam structure, TPTBL **5** and **5a** were expected to act as good acceptors. Both were brominated for further functionalization to produce the brominated TPTLs **6** and **6a**. Various donors were incorporated to generate the TPTBL-based D−A conjugated polymers. Three different types of donor monomers, 3,4-dodecylthiophene (DT, **7**), 4,4′-didodecyl-2,2′-bithiophene (DBT, **8**), and ethylenedioxythiophene (EDOT, **9**), were used, resulting in DT-TPTBL (**P1**), DBT-TPTBL (**P2**), and EDOT-TPTBL (**P3**), respectively. The donor strength was expected to increase in the order DT < DBT < EDOT, with the alkyl groups on the thiophene unit (**7** and **8**) needed to produce the soluble D−A conjugated polymers (**P1** and **P2**). In the case of EDOT, the branched 2-hexyl-1-decyl substituents on TPTBL **5a** were needed for the solubility of polymer **P3**.

We have extended the direct arylation reactions to the synthesis of polymers using the brominated TPTL acceptors (**6** and **6a**) and various donors (**7**, **8**, and **9**) (Scheme 2). Reacting the brominated TPTBL with the nonactivated thiophene

Scheme 2. Synthesis of the Thiophene−Phenylene−Thiophene Fused Bislactam (TPTBL)-Based Donor−Acceptor Polymers (P1, P2, and P3)

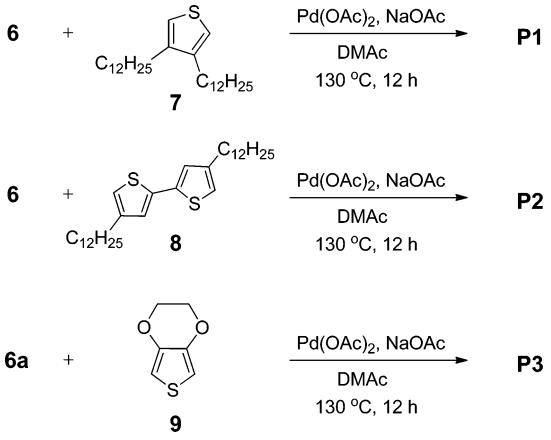

dx.doi.org/10.1021/ma4018907 | Macromolecules XXXX, XXX, XXX−XXX

derivatives (**7**, **8**, and **9**) in the presence of catalytic amounts of $Pd(OAc)_2$ and NaOAc as a base in DMAc at 130 °C provided the desired TPTBL-based alternating copolymers. Here the polycondensation by direct arylation was carried out in phosphine-free systems, eliminating the purification step to remove the problematic phosphine compounds after the reactions. Decomposed phosphine compounds are often incorporated into the main chain of conjugated polymers during polycondensation.[36,57,58] In addition, using the alkyl substituents at the β-position in thiophene derivatives of the donor components was expected to avoid the side reactions at the β-position of thiophene for direct arylation/polycondensation reaction, yielding highly regioregular polymers. Recently, a similar approach using β-substituted thiophene derivatives was employed to generate regioregular thiophene-based alternating copolymers.[9d] Since only a few backbone defects can significantly compromise their electronic structure and solid-state properties, regioregularity is indeed advantegeous in the synthesis of π-conjugated polymers. The analysis of polymer structure was difficult, however, because all the peaks on ^{1}H NMR spectra were too broad.

The polymers obtained had moderate molecular weights (Table 1) and were readily soluble in most organic solvents, including tetrahydrofuran, chloroform, and chlorobenzene.[59] TGA analysis showed thermal stability up to 420 °C for **P1**, 360 °C for **P2**, and 260 °C for **P3**, above which temperatures they started to degrade. DSC showed no characteristic thermal transition between 0 and 260 °C.

Table 1. Molecular Weight (GPC) Data for Polymers P1, P2, and P3

	M_n (kDa)	M_w (kDa)	PDI
P1	7.6	14.8	1.9
P2	8.9	24.0	2.7
P3	8.2	18.8	2.3

3.2. Electronic and Molecular Structures. To analyze the geometric changes induced by different donor groups with varying steric properties, DFT calculations were performed on the monomeric building blocks of each copolymer. Figure 1 shows the optimized geometries and the predicted frontier molecular orbital energy levels for each model. The higher degree of steric crowding was observed for polymer **P1**, whose donor thiophene ring is substituted with alkyl chains in both its β-positions. This crowding resulted in a dihedral angle of around 41° between the donor and acceptor groups. The release of one of these alkyl groups greatly diminishes the steric hindrance, making the aforementioned dihedral angle more planar, with a value of 24° for **P2**. Furthermore, substitution at the thiophenic β-positions by an ethylenedioxy group (EDOT) in **P3** results in the conjugated backbone becoming completely planar due to the appearance of intramolecular S···O interactions.[60−62] These interactions are evidenced by theoretical calculations, which predict a sulfur−oxygen distance of 2.96 Å, while the sum of their van der Waals radii amounts to 3.32 Å. These findings suggest that π-conjugation is enhanced due to molecular planarity on passing from **P1** to **P3**. This enhanced planarity/rigidity may be beneficial for their application in electronic devices.[63]

These findings are in good agreement with the UV−vis optical data (see Figure 2 and Table 2), which showed a displacement of the absorption maximum (483, 502, and 529 nm for **P1**, **P2**, and **P3**, respectively) as planarity was increased and in the presence of a highly electron-rich EDOT group in the case of polymer **P3**. The same red-shift was observed for thin film spectra, with values of 503, 510, and 540 nm for **P1**, **P2**, and **P3**, respectively. The wavelength displacement on passing from solution to film indicates favorable aggregation in the thin films. In addition, the occurrence of intramolecular interactions that provoke polymer backbone rigidity is also evident in the absorption spectra profiles (Figure 2). Note that the **P3** solution spectrum presents quite

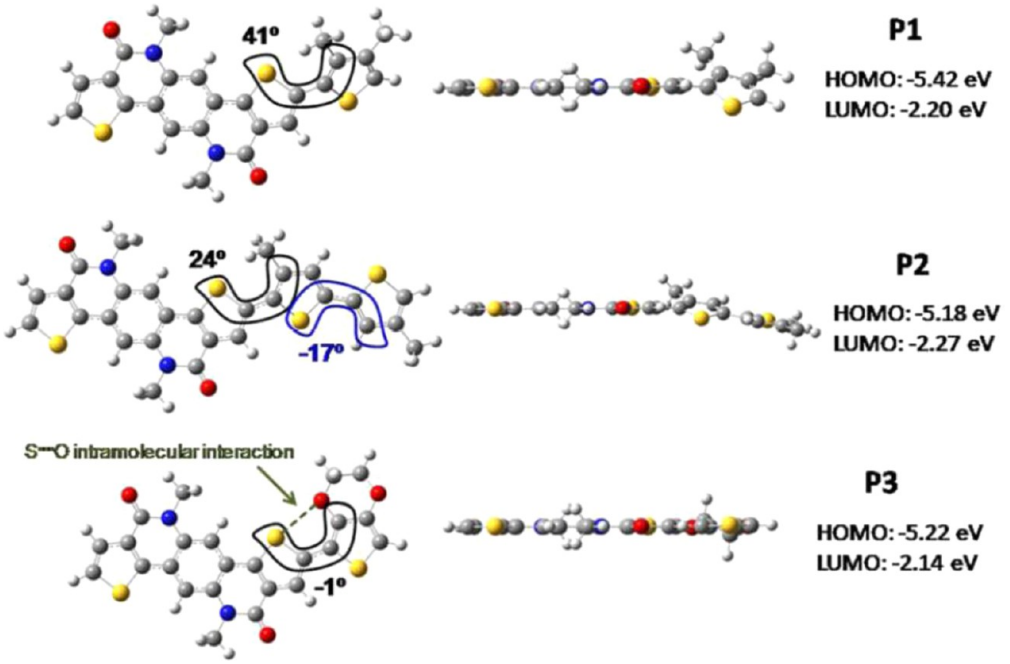

Figure 1. DFT//B3LYP/6-31G** optimized structures and estimated HOMO and LUMO energies for the studied polymeric building blocks. Alkyl substituents were replaced by methyl groups to simplify the calculations.

dx.doi.org/10.1021/ma4018907 | *Macromolecules* XXXX, XXX, XXX−XXX

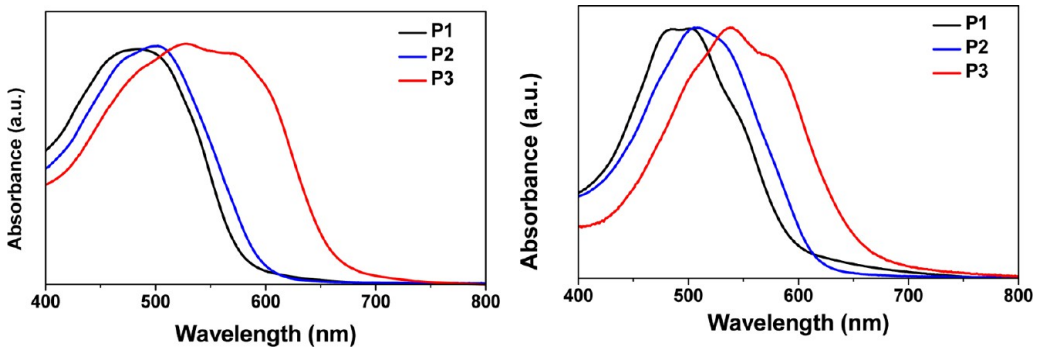

Figure 2. UV−vis absorption spectra of polymer solution (in chloroform) (left) and thin films (right).

Table 2. Optical and Electrochemical Properties of the Indicated Polymers[a]

	λ_{max} (nm) solution	λ_{max} (nm) film	E^{opt} (eV)	E^{ox}(onset) (eV)	E^{red}(onset) (eV)	HOMO (eV)	LUMO (eV)	E_g (eV)
P1	483	503	2.05	1.23	−0.80	−5.67	−3.64	2.03
P2	502	510	1.96	0.91	−1.18	−5.35	−3.49	1.86
P3	529	540, 570	1.83	0.93	−0.85	−5.37	−3.59	1.78

[a]The optical data were analyzed in chloroform while the electrochemistry (V versus SCE) of the polymeric thin films was performed in acetonitrile. The frontier molecular orbital energies were calculated from the cyclic voltammetry data.

evident vibronic structure, indicating skeletal rigidity due to the S···O attractive interaction.[64]

An efficient field effect transistor requires the semiconducting material to possess appropriate HOMO and/or LUMO energies to facilitate hole (p-type)[47,48] and/or electron (n-type)[27,65,66] injection from the electrode, to optimize charge transport in the device channel, and to enhance device environmental stability.[48,65] We therefore assessed the electrochemical properties of polymers **P1**−**P3** as thin films in a solution of 0.1 M tetrabutylammonium hexafluorophosphate in acetonitrile under a nitrogen flow and at a scan rate of 100 mV/s. Platinum electrodes were used as both the working and the counter electrodes, and an Ag wire was used as the pseudoreference electrode. Polymer films were drop cast onto the platinum working electrode from a concentrated chloroform solution. Ferrocene/ferrocinium (Fc/Fc^+) was used as an internal reference to report the potential versus SCE, which has an energy of −4.44 eV below the vacuum level.[67] The frontier orbital energy levels of **P1**−**P3** were determined from the oxidation/reduction onsets of the cyclic voltammetry curves and calculated according to the equations

$$E_{HOMO} = -(E_{ox}^{onset} + 4.44)\ (eV)$$

$$E_{LUMO} = -(E_{red}^{onset} + 4.44)\ (eV)$$

Table 2 summarizes the optical and electrochemistry data for the three polymers. Note that there was remarkable agreement between the optical and electrochemically derived energy gaps. These data were utilized to calculate the HOMO and LUMO energies. The proximity of the HOMO energy levels of the polymer to the −5.0 eV Fermi level of the gold electrode anticipates efficient charge injection in the device. However, once the hole/electron is injected, the charge should be stabilized in the channel and then should be able to hop from molecule to molecule to reach the drain electrode. In this sense, a theoretical parameter that accounts for the structural reorganization needed when a hole/electron is transferred between two neighboring molecules is the intramolecular reorganization energy as defined in the Marcus theory of electron transfer.[68] This energetic parameter diminishes as the conjugated skeleton becomes more rigid, with values of 0.33, 0.27, and 0.24 eV for **P1**, **P2**, and **P3**, respectively.

The molecular structures of the polymers were also analyzed by Raman vibrational spectroscopy. Figure 3 shows the FT-

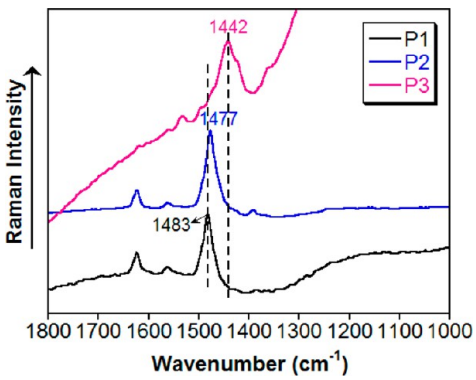

Figure 3. FT-Raman spectra (λ_{exc}: 1064 nm) of the polymers **P1**−**P3** in the solid state.

Raman spectra for these three polymers in solid state. (The DFT predicted spectra and selected eigenvectors are shown in the Supporting Information.) The spectra are characterized by very simple profiles, with each having only a few intense bands. The most intense band in the **P1** spectrum is located at 1483 cm^{-1} and corresponds to a collective vibration of the lactam core units, without an appreciable contribution from the dialkyl-substituted thiophene comonomer. In this normal mode, the thiophenic C═C double bonds lengthen in phase while the C−C single bonds shrink in phase, describing the elongation of the π-conjugation throughout the polymeric chain. This normal mode downshifts to 1477 cm^{-1} in **P2**. In this case, the vibration is delocalized over the whole conjugated skeleton with noticeable contribution of the alkyl-substituted bithiophene counit.

This delocalized vibration and its frequency downshift with respect to **P1** indicate that there exists a more efficient communication in **P2** between the two comonomeric units, resulting in enhanced π-conjugation, as indicated by the more

dx.doi.org/10.1021/ma4018907 | *Macromolecules* XXXX, XXX, XXX−XXX

planar skeleton predicted by DFT calculations. In **P3**, this band is further downshifted to 1442 cm^{-1}, in agreement with the more conjugated skeleton found both by quantum chemical predictions and optical spectroscopic data. However, the theoretical spectrum does not track the frequency downshift for polymer **P3** (see Supporting Information). These calculations were performed on isolated molecules in a vacuum, which omit the strong intermolecular interactions expected for this planar polymer which produce enhanced π-conjugation.

3.3. Photophysical Analysis. Figure 4 displays the absorption, excitation, and emission spectra of the three polymers. As we have previously shown, the absorption spectra are characterized by a single intense absorption above 350 nm, which is downshifted as the conjugated skeleton becomes more planar and a stronger donor is used. Excitation at the maximum wavelength resulted in an emission spectrum for each polymer, characterized by a broad and unresolved shape for **P1**. In marked contrast, the emission spectra of polymers **P2** and **P3** display vibronic structure, indicating a more rigid structure of their emitting excited state: in **P2** this emitting state is rigidified by the quinoidization of the bithiophene core, while in **P3** it is already planar by the S···O coupling. **P1** with a monomeric thiophene provides residual quinoidization to the excited state.

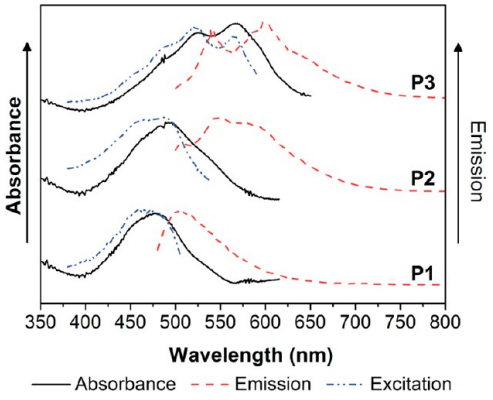

Figure 4. Absorption, emission, and excitation spectra for polymers **P1**–**P3**.

Figure 5 shows the transient absorption spectra of the three polymers in microseconds regime after excitation. In all three polymers, the ground electronic state absorption becomes depleted, with the emergence of new bands at longer wavelengths. Well-defined isosbestic points for **P1** and **P2** are observed, suggesting the reversible interconversion between the ground state and the excited state without noticeable degradation. For polymer **P3** the isosbestic point is not perfectly clear. The lifetimes of the photoexcited species for all three polymers are around 20 μs, indicating the formation of an absorbing triplet species after laser pulse excitation. The transient triplet–triplet absorption spectra for these polymers are broad, suggesting some delocalization of the triplet excited-state resulting from an effective conjugation along the copolymer backbone.[69] Furthermore, the appearance of these triplet species in these polymers after laser excitation can be related with their photovoltaic activity[70] in the sense that the formation of long-lived triplets might compete with charge transfer singlet excitons.[71] Therefore, the presence of the triplets in these polymers might act against the overall yield of charge generation on one hand and also might open undesiderable routes for chemical degradation in photovoltaic cells.

3.4. Thin Film Characterization. To understand the effects of the different donor comonomers, the various skeletal planarities, and the effect of alkyl chain substitution[64,72] on the electrical performance of the donor–acceptor polymers, it was

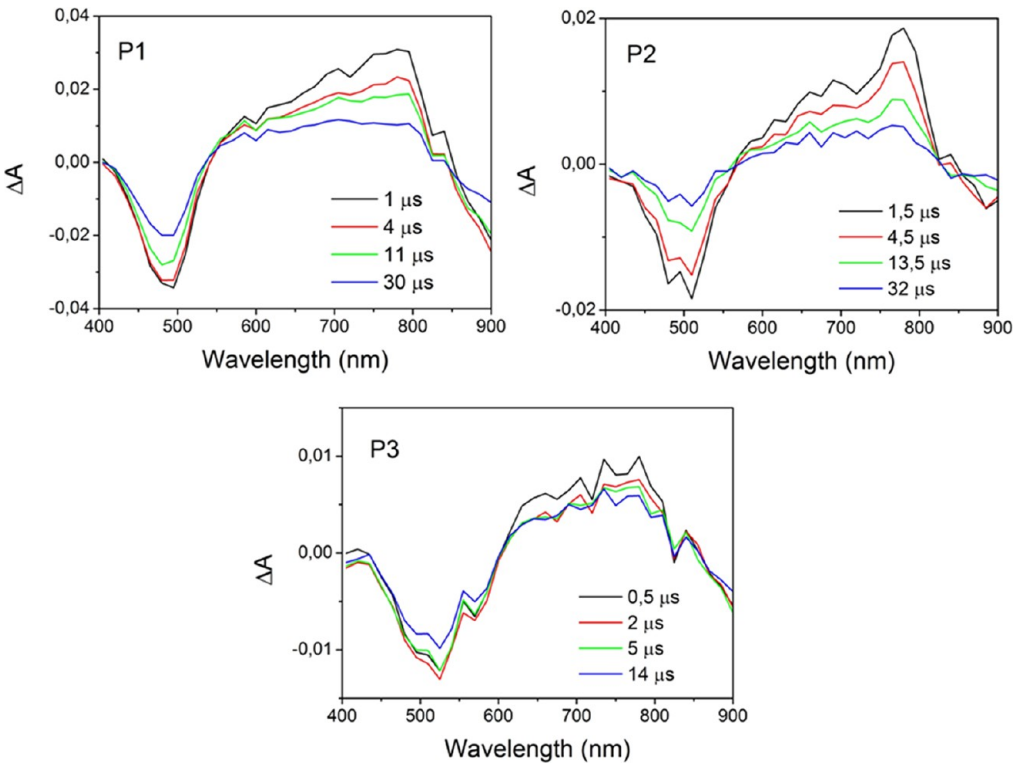

Figure 5. Transient absorption spectra recorded for polymers **P1**–**P3**.

dx.doi.org/10.1021/ma4018907 | *Macromolecules* XXXX, XXX, XXX–XXX

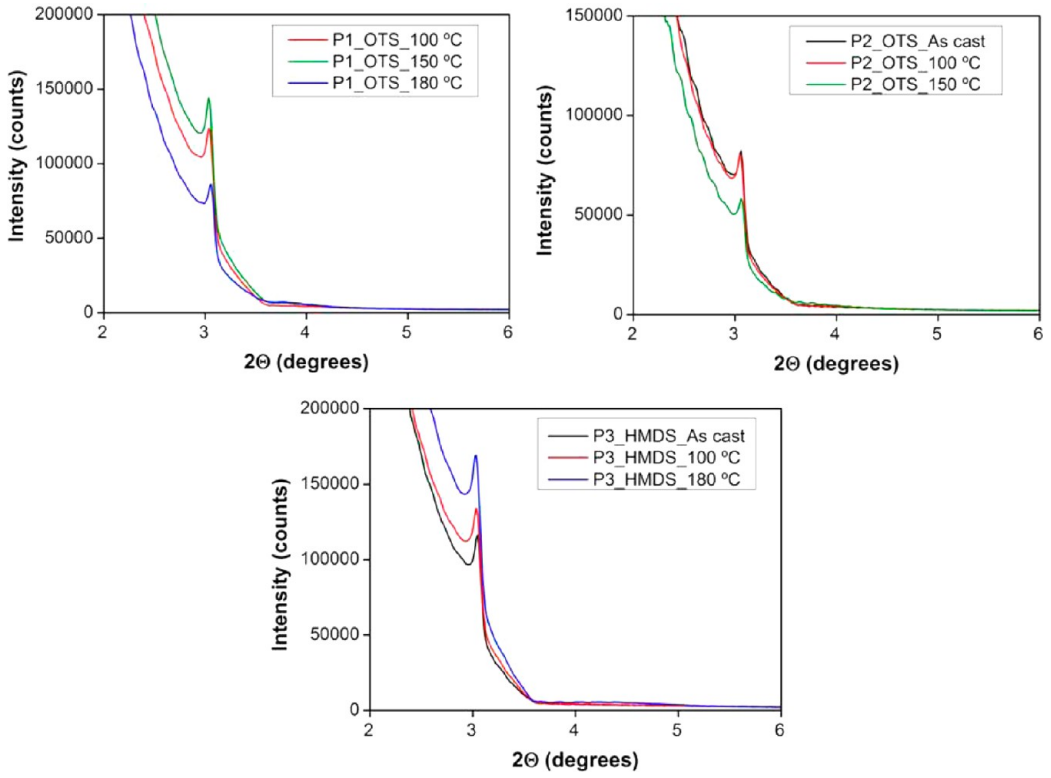

Figure 6. Out-of-plane X-ray diffraction spectra (XRD) recorded for **P1**−**P3** drop-cast on a modified Si/SiO_2 wafer after annealing at different temperatures. HMDS: films deposited on hexamethyldisilazane-treated substrates; OTS: films deposited on octadecyltrichlorosilane-treated substrates.

necessary to analyze the microstructures and surface morphologies of the thin films used for device fabrication. Effective intermolecular charge transport in thin film requires the polymer chain to align closely and uniformly. Furthermore, the optimal orientation is that in which cofacial π-conjugated planes are aligned in the source-drain direction (edge-on orientation), perpendicular to the substrate surface.[73,74] The molecular orientation of the polymers was then studied by small-angle X-ray diffraction (SAX) (Figure 6). The polymers were spin-cast over OTS-modified silicon wafer and annealed at different temperatures for 2 h before scanning. After the annealing process, the samples were left to cool down slowly under vacuum. All three polymers showed a unique first-order (100) diffraction peak, which indicates that the polymer thin films are not highly crystalline. All of the polymers show their primary diffraction at around a 2θ value of 3°, making their corresponding d-spacings 28.9 Å. The appearance of these (100) peaks in all the systems indicates a lamellar alignment of the three polymeric chains, an alignment typically observed for high performance solution processable conjugated polymers. However, no second-order diffraction peaks are recorded, which points out the absence of noticeable long-range crystallinity. It should be also noted that there is no evidence of appreciable $\pi-\pi$ stacking in any of the samples.

Polymers **P1** and **P3** are the ones showing the most intense diffraction peaks, while **P2** thin films present lower crystallinity. As shown in Figure 6, a moderate annealing treatment (100 or 150 °C) on **P1** thin films induces an enhancement of the (100) peak intensity. However, annealing at a higher temperature (180 °C) diminishes the film crystallinity (the intensity of the (100) peak varies from ∼150 000 counts at 150 °C to ∼87 000 counts at 180 °C). For **P2** thin films a similar trend is found, being the sample annealed at higher temperature the one showing the lowest crystallinity. In contrast, for **P3**, the (100) peak intensity is gradually enhanced upon increasing the annealing temperature.

Analysis of thin films was completed by the acquisition of AFM images (Figure 7). AFM is a technique frequently used to shed light on the TFT dielectric−semiconductor interface, although in principle it is unable to directly characterize it. However, superficial AFM is used to assess the microstructural properties of the active region of a thin film transistor.

Figure 7 shows that the **P1** polymer yields the most textured films within the polymeric family, with the appearance of small and round grains. Moreover, its crystallinity was enhanced by increasing the annealing temperature from 25 °C up to 150 °C, but was substantially damaged at higher values. In fact, the AFM of **P1** thin film annealed at 180 °C shows degraded crystallinity, which is in complete agreement with the XRD data. Furthermore, they also show a rougher surface, indicating a less homogeneous film. **P2** shows a similar behavior, whereas **P3** thin film AFM images indicate smaller crystalline grains.[75]

3.5. Device Fabrication and Characterization. Bottom-gate top-contact OTFTs were fabricated to investigate the charge transport properties of the **P1**−**P3** polymers. Table 3 shows the average OFET performances, while Figure 8 shows selected output and transfer plots.

Note from Table 3 that only **P2** and **P3** were active in OFETs, although their performances were quite low. For **P2** deposited on OTS-treated substrates and annealed at 150 °C, the average recorded hole mobility was 1.4×10^{-5} $cm^2\,V^{-1}\,s^{-1}$, with a threshold voltage of −29 V and a very low on/off ratio of ∼20. In contrast, **P3** was active under a variety of tested conditions, with the best performance achieved by films deposited on OTS-treated substrates and annealed at 180 °C for 2 h, with an average field-effect mobility of $\sim 5 \times 10^{-5}$ $cm^2\,V^{-1}\,s^{-1}$, threshold voltage of −75 V, and an on/off ratio of 10^{+2}. Lower annealing

dx.doi.org/10.1021/ma4018907 | *Macromolecules* XXXX, XXX, XXX−XXX

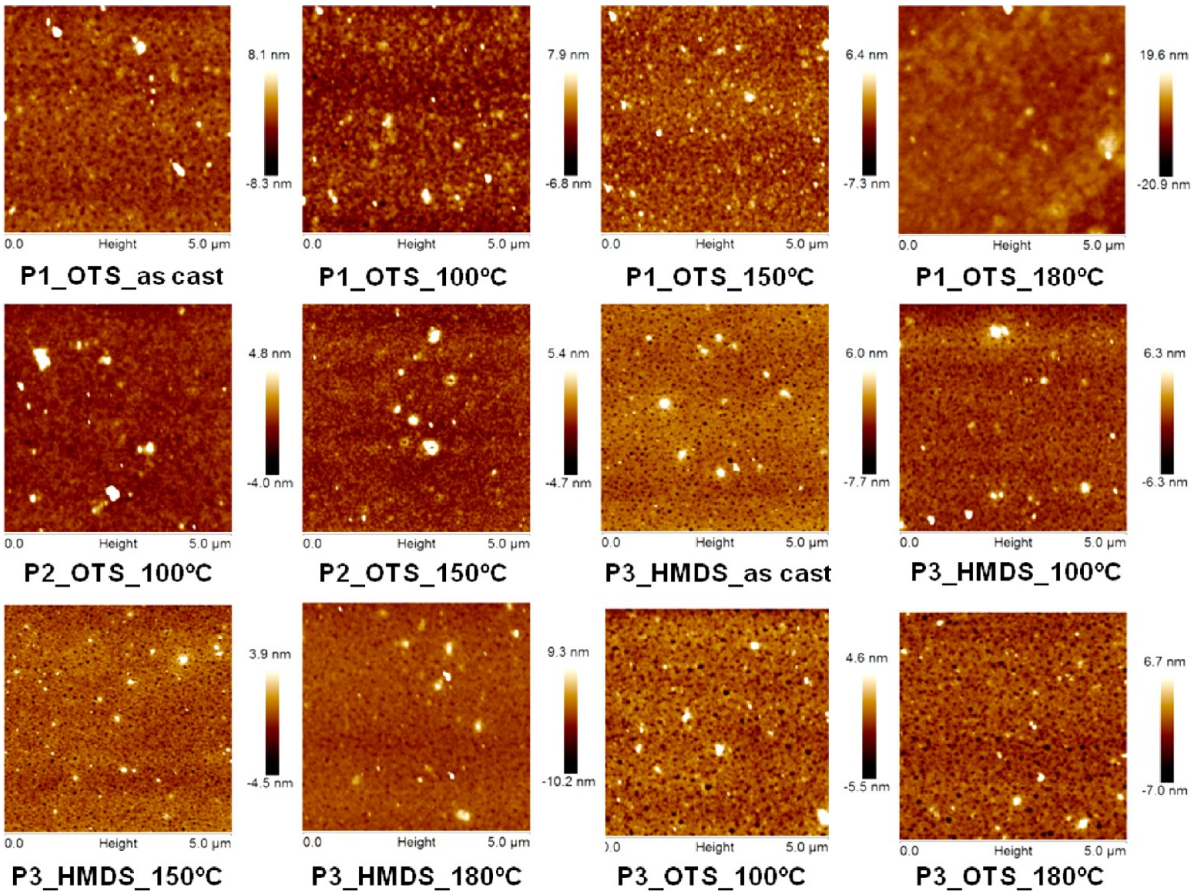

Figure 7. AFM images of spin-cast thin films of **P1**−**P3** polymers annealed at the indicated temperatures. Image size: 5 × 5 μm. HMDS: films deposited on hexamethyldisilazane-treated substrates; OTS: films deposited on octadecyltrichlorosilane-treated substrates.

Table 3. Summary of OFET Electrical Data for Spin-Cast Polymeric Films Annealed at the Indicated Temperatures and Measured in Ambient Conditions

polymer	substrate	annealing temp (°C)	μ_h ($cm^2\ V^{-1}\ s^{-1}$)	V_T (V)	I_{ON}/I_{OFF}
P2	OTS	150	1.4×10^{-5}	−29	∼20
P3	OTS	100	2.2×10^{-5}	7	∼10
P3	HMDS	150	1.1×10^{-5}	17	∼10
P3	OTS	150	4.1×10^{-6}	−77	∼20
P3	HMDS	180	2.5×10^{-5}	−70	10^{+2}
P3	OTS	180	4.8×10^{-5}	−75	10^{+2}

temperatures are translated into slightly deteriorated electrical performances. This can be related with the enhancement of **P3** thin film crystallinity, found in XRD spectra, with higher temperature treatments.

In terms of molecular and electronic structures, the higher field effect performance of **P3** versus **P2** is expected due to the extended π-conjugation (as indicated by FT-Raman spectroscopy) and lower intramolecular reorganization energy of the former. Furthermore, XRD also indicates enhanced crystallinity for **P3** thin films, probably due to the more planar skeleton induced by the appearance of intramolecular S···O interactions. Therefore, we assume, that in the case of **P3**, TFT performance is

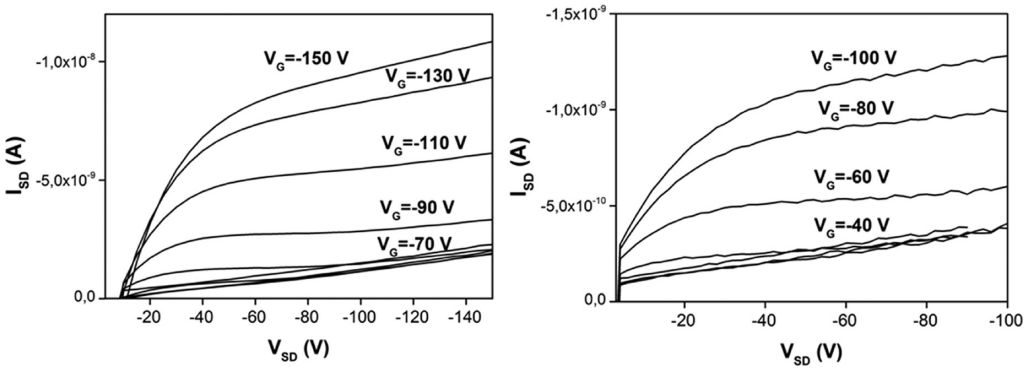

Figure 8. OTFT output characteristics of a **P3** film deposited on an OTS-treated substrate and annealed at 180 °C (left) and of a **P2** film deposited on an OTS-treated substrate and annealed at 150 °C (right).

dx.doi.org/10.1021/ma4018907 | *Macromolecules* XXXX, XXX, XXX−XXX

improved respect to the other two polymers probably to both higher crystallinity films and to the occurrence of a better interchain delocalization (induced by a more planar π-skeleton), which promotes transport from source to drain by charge hopping between adjacent polymeric chains.

In the case of **P1** and **P2** polymers, focusing solely on thin film microstructures, one should expect **P1** to perform better than **P2**, due to enhanced crystallinity. However, **P1** is not active under none of the conditions tested. Note however that **P1** HOMO energy level is stabilized in approximately 0.3 eV with respect to **P2** and **P3** due to the predicted skeletal distortion; that is translated in a higher energy barrier for hole injection from the gold electrodes (Fermi level of gold is ~−5.0 eV), which could be one of the reasons behind the **P1** inactivity.

4. CONCLUSIONS

We prepared a series of new donor−acceptor copolymer semiconductors based on thiophene−phenylene−thiophene fused bislactam (TPTBL) and various donor moieties by polycondensation using direct C−H arylation of thiophene derivatives with brominated TPTBL. This method is advantageous compared with traditional cross-coupling polymerization since it requires fewer synthetic operations and does not employ toxic organometallic intermediates. Regioselective polymers are also expected by the use of β-substituted thiophene derivative compounds.

Using this approach, we synthesized three different donor−acceptor polymers with varying electrical performances. In this series, careful selection of the donor unit allowed bandgap engineering, which was dictated both by the intrinsic electronic properties of the donor unit and by the appearance of intramolecular attractive/repulsive (steric) interactions. The electrical performances of the studied polymers were analyzed in a TFT architecture, with the best performance displayed by the **P3** polymer, which presented the highest conjugation within the series, highest crystallinity, and lower intramolecular reorganization energies. However, thin film analysis showed that this polymer is not highly crystalline as only one XRD peak is recorded, which is probably one of the reasons for its low performance.

■ ASSOCIATED CONTENT

Supporting Information

Copies of NMR spectra for all the compounds and additional theoretical data. This material is available free of charge via the Internet at http://pubs.acs.org.

■ AUTHOR INFORMATION

Corresponding Authors

*E-mail teodomiro@uma.es; Fax (34)-952132018 (L.N.).
*E-mail rocioponce@uma.es; Fax (34)-952131863 (R.P.O.).
*E-mail tkim@incheon.ac.kr; Fax (82)-32-8350762 (T.-H.K.).

Notes

The authors declare no competing financial interest.

■ ACKNOWLEDGMENTS

Part of this work was supported by the Incheon National University International Cooperative Research Grant in 2011. We also thank MINECO (CTQ2012-33733) for support at University of Malaga. R.P.O. thanks MINECO for a "Ramón y Cajal" research contract. Dr. Ute Zschieschang is greatly acknowledged for her support during gold deposition.

■ REFERENCES

(1) Facchetti, A. *Chem. Mater.* **2011**, *23*, 733−758.
(2) Marks, T. J. *MRS Bull.* **2010**, *35*, 1018−1027.
(3) Sun, J.; Zhang, B.; Katz, H. E. *Adv. Funct. Mater.* **2011**, *21*, 29−45.
(4) Wolfer, P.; Santarelli, M. L.; Vaccaro, L.; Yu, L.; Anthopoulos, T. D.; Smith, P.; Stingelin, N.; Marrocchi, A. *Org. Electron.* **2011**, *12*, 1886−1892.
(5) Anthony, J. E.; Facchetti, A.; Heeney, M.; Marder, S. R.; Zhan, X. W. *Adv. Mater.* **2010**, *22*, 3876−3892.
(6) Tang, C. W.; VanSlyke, S. A.; Chen, C. H. *J. Appl. Phys.* **1989**, *65*, 3610−3616.
(7) Grimsdale, A. C.; Leok Chan, K.; Martin, R. E.; Jokisz, P. G.; Holmes, A. B. *Chem. Rev.* **2009**, *109*, 897−1091.
(8) Coropceanu, V.; Cornil, J.; da Silva Filho, D. A.; Olivier, Y.; Silbey, R.; Brédas, J.-L. *Chem. Rev.* **2007**, *107*, 926−952.
(9) Mas-Torrent, M.; Rovira, C. *Chem. Soc. Rev.* **2008**, *37*, 827−838.
(10) Wu, W.; Liu, Y.; Zhu, D. *Chem. Soc. Rev.* **2010**, *39*, 1489−1502.
(11) Allard, S.; Forster, M.; Souharce, B.; Thiem, H.; Scherf, U. *Angew. Chem., Int. Ed.* **2008**, *47*, 4070−4098.
(12) Ooyama, Y.; Harima, Y. *Eur. J. Org. Chem.* **2009**, *2009*, 2903−2934.
(13) Mishra, A.; Fischer, M. K. R.; Bäuerle, P. *Angew. Chem., Int. Ed.* **2009**, *48*, 2474−2499.
(14) Ning, Z.; Tian, H. *Chem. Commun.* **2009**, 5483−5495.
(15) Alberico, D.; Scott, M. E.; Lautens, M. *Chem. Rev.* **2007**, *107*, 174−238.
(16) Kim, I.; Yoo, M.; Kim, T.-H. *Tetrahedron* **2007**, *63*, 9476−9481.
(17) Ong, B. S.; Wu, Y.; Liu, P.; Gardner, S. *J. Am. Chem. Soc.* **2004**, *126*, 3378−3379.
(18) Wu, Y.; Liu, P.; Gardner, S.; Ong, B. S. *Chem. Mater.* **2004**, *17*, 221−223.
(19) McCullough, R. D. *Adv. Mater.* **1998**, *10*, 93−116.
(20) Sirringhaus, H.; Wilson, R. J.; Friend, R. H.; Inbasekaran, M.; Wu, W.; Woo, E. P.; Grell, M.; Bradley, D. D. C. *Appl. Phys. Lett.* **2000**, *77*, 406−408.
(21) McCulloch, I.; Heeney, M.; Bailey, C.; Genevicius, K.; MacDonald, I.; Shkunov, M.; Sparrowe, D.; Tierney, S.; Wagner, R.; Zhang, W.; Chabinyc, M. L.; Kline, R. J.; McGehee, M. D.; Toney, M. F. *Nat. Mater.* **2006**, *5*, 328−333.
(22) Kong, H.; Jung, Y. K.; Cho, N. S.; Kang, I.-N.; Park, J.-H.; Cho, S.; Shim, H.-K. *Chem. Mater.* **2009**, *21*, 2650−2660.
(23) Cheedarala, R. K.; Kim, G.-H.; Cho, S.; Lee, J.; Kim, J.; Song, H.-K.; Kim, J. Y.; Yang, C. *J. Mater. Chem.* **2011**, *21*, 843−850.
(24) Blouin, N.; Michaud, A.; Gendron, D.; Wakim, S.; Blair, E.; Neagu-Plesu, R.; Belletête, M.; Durocher, G.; Tao, Y.; Leclerc, M. *J. Am. Chem. Soc.* **2007**, *130*, 732−742.
(25) Zhou, W.; Wen, Y.; Ma, L.; Liu, Y.; Zhan, X. *Macromolecules* **2012**, *45*, 4115−4121.
(26) Zhan, X.; Facchetti, A.; Barlow, S.; Marks, T. J.; Ratner, M. A.; Wasielewski, M. R.; Marder, S. R. *Adv. Mater.* **2011**, *23*, 268−284.
(27) Yan, H.; Chen, Z. H.; Zheng, Y.; Newman, C.; Quinn, J. R.; Dotz, F.; Kastler, M.; Facchetti, A. *Nature* **2009**, *457*, 679−U1.
(28) McGlacken, G. P.; Bateman, L. M. *Chem. Soc. Rev.* **2009**, *38*, 2447−2464.
(29) Majumdar, K. C.; De, N.; Chakravorty, S. *Synth. Commun.* **2010**, *41*, 121−130.
(30) Campeau, L.-C.; Parisien, M.; Leblanc, M.; Fagnou, K. *J. Am. Chem. Soc.* **2004**, *126*, 9186−9187.
(31) Stuart, D. R.; Fagnou, K. *Science* **2007**, *316*, 1172−1175.
(32) Gorelsky, S. I.; Lapointe, D.; Fagnou, K. *J. Am. Chem. Soc.* **2008**, *130*, 10848−10849.
(33) Sévignon, M.; Papillon, J.; Schulz, E.; Lemaire, M. *Tetrahedron Lett.* **1999**, *40*, 5873−5876.
(34) Schipper, D. J.; Fagnou, K. *Chem. Mater.* **2011**, *23*, 1594−1600.
(35) Lu, W.; Kuwabara, J.; Kanbara, T. *Macromolecules* **2011**, *44*, 1252−1255.
(36) Fujinami, Y.; Kuwabara, J.; Lu, W.; Hayashi, H.; Kanbara, T. *ACS Macro Lett.* **2011**, *1*, 67−70.

(37) van Mullekom, H. A. M.; Vekemans, J. A. J. M.; Havinga, E. E.; Meijer, E. W. *Mater. Sci. Eng., R* **2001**, *32*, 1−40.
(38) Jenekhe, S. A.; Lu, L.; Alam, M. M. *Macromolecules* **2001**, *34*, 7315−7324.
(39) Pron, A.; Gawrys, P.; Zagorska, M.; Djurado, D.; Demadrille, R. *Chem. Soc. Rev.* **2010**, *39*, 2577−2632.
(40) Zhu, Y.; Kulkarni, A. P.; Wu, P.-T.; Jenekhe, S. A. *Chem. Mater.* **2008**, *20*, 4200−4211.
(41) Brédas, J.-L.; Norton, J. E.; Cornil, J.; Coropceanu, V. *Acc. Chem. Res.* **2009**, *42*, 1691−1699.
(42) Zaumseil, J.; Donley, C. L.; Kim, J. S.; Friend, R. H.; Sirringhaus, H. *Adv. Mater.* **2006**, *18*, 2708−2712.
(43) Chua, L. L.; Zaumseil, J.; Chang, J. F.; Ou, E. C. W.; Ho, P. K. H.; Sirringhaus, H.; Friend, R. H. *Nature* **2005**, *434*, 194−199.
(44) Yamamoto, T.; Yasuda, T.; Sakai, Y.; Aramaki, S.; Ramaw, A. *Macromol. Rapid Commun.* **2005**, *26*, 1214−1217.
(45) Zhu, Y.; Champion, R. D.; Jenekhe, S. A. *Macromolecules* **2006**, *39*, 8712−8719.
(46) Champion, R. D.; Cheng, K.-F.; Pai, C.-L.; Chen, W.-C.; Jenekhe, S. A. *Macromol. Rapid Commun.* **2005**, *26*, 1835−1840.
(47) Guo, X.; Ortiz, R. P.; Zheng, Y.; Hu, Y.; Noh, Y.-Y.; Baeg, K.-J.; Facchetti, A.; Marks, T. J. *J. Am. Chem. Soc.* **2011**, *133*, 1405−1418.
(48) Guo, X.; Ortiz, R. P.; Zheng, Y.; Kim, M.-G.; Zhang, S.; Hu, Y.; Lu, G.; Facchetti, A.; Marks, T. J. *J. Am. Chem. Soc.* **2011**, *133*, 13685−13697.
(49) Letizia, J. A.; Salata, M. R.; Tribout, C. M.; Facchetti, A.; Ratner, M. A.; Marks, T. J. *J. Am. Chem. Soc.* **2008**, *130*, 9679−9694.
(50) Zhan, X.; Tan, Z. a.; Domercq, B.; An, Z.; Zhang, X.; Barlow, S.; Li, Y.; Zhu, D.; Kippelen, B.; Marder, S. R. *J. Am. Chem. Soc.* **2007**, *129*, 7246−7247.
(51) Zou, Y.; Najari, A.; Berrouard, P.; Beaupré, S.; Réda Aïch, B.; Tao, Y.; Leclerc, M. *J. Am. Chem. Soc.* **2010**, *132*, 5330−5331.
(52) Bürgi, L.; Turbiez, M.; Pfeiffer, R.; Bienewald, F.; Kirner, H.-J.; Winnewisser, C. *Adv. Mater.* **2008**, *20*, 2217−2224.
(53) Becke, A. D. *J. Chem. Phys.* **1993**, *98*, 1372.
(54) Francl, M. M.; Pietro, W. J.; Hehre, W. J.; Binkley, J. S.; Gordon, M. S.; Defrees, D. J.; Pople, J. A. *J. Chem. Phys.* **1982**, *77*, 3654.
(55) Frisch, M. J.; Trucks, G. W.; Schlegel, H. B.; Scuseria, G. E.; Robb, M. A.; Cheeseman, J. R.; Scalmani, G.; Barone, V.; Mennucci, B.; Petersson, G. A.; Nakatsuji, H.; Caricato, M.; Li, X.; Hratchian, H. P.; Izmaylov, A. F.; Bloino, J.; Zheng, G.; Sonnenberg, J. L.; Hada, M.; Ehara, M.; Toyota, K.; Fukuda, R.; Hasegawa, J.; Ishida, M.; Nakajima, T.; Honda, Y.; Kitao, O.; Nakai, H.; Vreven, T.; Montgomery, J.; Peralta, J. E.; Ogliaro, F.; Bearpark, M.; Heyd, J. J.; Brothers, E.; Kudin, K. N.; Staroverov, V. N.; Kobayashi, R.; Normand, J.; Raghavachari, K.; Rendell, A.; Burant, J. C.; Iyengar, S. S.; Tomasi, J.; Cossi, M.; Rega, N.; Millam, J. M.; Klene, M.; Knox, J. E.; Cross, J. B.; Bakken, V.; Adamo, C.; Jaramillo, J.; Gomperts, R.; Stratmann, R. E.; Yazyev, O.; Austin, A. J.; Cammi, R.; Pomelli, C.; Ochterski, J. W.; Martin, R. L.; Morokuma, K.; Zakrzewski, V. G.; Voth, G. A.; Salvador, P.; Dannenberg, J. J.; Dapprich, S.; Daniels, A. D.; Farkas, Ö.; Foresman, J. B.; Ortiz, J. V.; Cioslowski, J.; Fox, D. J. *Gaussian 09, Revision C.01*, Gaussian, Inc.: Wallingford, CT, 2010.
(56) Walter, S. R.; Youn, J.; Emery, J. D.; Kewalramani, S.; Hennek, J. W.; Bedzyk, M. J.; Facchetti, A.; Marks, T. J.; Geiger, F. M. *J. Am. Chem. Soc.* **2012**, *134*, 11726−11733.
(57) Goodson, F. E.; Wallow, T. I.; Novak, B. M. *Macromolecules* **1998**, *31*, 2047−2056.
(58) Goodson, F. E.; Hauck, S. I.; Hartwig, J. F. *J. Am. Chem. Soc.* **1999**, *121*, 7527−7539.
(59) For comparison, the polymer **P2** was also prepared by the classical Suzuki coupling reaction from the corresponding diboronic ester and monomer **6**. The Suzuki-polymerized **P2*** showed slightly lower molecular weight (M_n of 6.8 kDa) than the direct arylation-polymerized **P2** (M_n of 8.9 kDa), possibly due to the loss of some functional groups during the Suzuki polymerization. Similar results were also reported. See: Berrouard, P.; Najari, A.; Pron, A.; Gendron, D.; Morin, P.-O.; Pouliot, J.-R.; Veilleux, J.; Leclerc, M. *Angew. Chem., Int. Ed.* **2012**, *51*, 2068−2071.
(60) Turbiez, M.; Frère, P.; Roncali, J. *J. Org. Chem.* **2003**, *68*, 5357−5360.
(61) Roncali, J.; Blanchard, P.; Frere, P. *J. Mater. Chem.* **2005**, *15*, 1589−1610.
(62) Turbiez, M.; Frère, P.; Allain, M.; Videlot, C.; Ackermann, J.; Roncali, J. *Chem.—Eur. J.* **2005**, *11*, 3742−3752.
(63) Lei, T.; Dou, J.-H.; Cao, X.-Y.; Wang, J.-Y.; Pei, J. *J. Am. Chem. Soc.* **2013**, *135*, 12168−12171.
(64) Guo, X.; Quinn, J.; Chen, Z.; Usta, H.; Zheng, Y.; Xia, Y.; Hennek, J. W.; Ortiz, R. P.; Marks, T. J.; Facchetti, A. *J. Am. Chem. Soc.* **2013**, *135*, 1986−1996.
(65) Zhao, Y.; Di, C.-a.; Gao, X.; Hu, Y.; Guo, Y.; Zhang, L.; Liu, Y.; Wang, J.; Hu, W.; Zhu, D. *Adv. Mater.* **2011**, *23*, 2448−2453.
(66) Jones, B. A.; Facchetti, A.; Wasielewski, M. R.; Marks, T. J. *J. Am. Chem. Soc.* **2007**, *129*, 15259−15278.
(67) Meerholz, K.; Heinze, J. *Electrochim. Acta* **1996**, *41*, 1839−1854.
(68) Malagoli, M.; Bredas, J. L. *Chem. Phys. Lett.* **2000**, *327*, 13−17.
(69) Pina, J.; Seixas de Melo, J.; Burrows, H. D.; Galbrecht, F.; Nehls, B. S.; Farrell, T.; Scherf, U. *J. Phys. Chem. C* **2007**, *111*, 7185−7191.
(70) Dufresne, S. p.; Roche, I. U.; Skalski, T.; Skene, W. G. *J. Phys. Chem. C* **2010**, *114*, 13106−13112.
(71) Köhler, A.; Bässler, H. *Mater. Sci. Eng., R* **2009**, *66*, 71−109.
(72) Zhang, F.; Hu, Y.; Schuettfort, T.; Di, C.-a.; Gao, X.; McNeill, C. R.; Thomsen, L.; Mannsfeld, S. C. B.; Yuan, W.; Sirringhaus, H.; Zhu, D. *J. Am. Chem. Soc.* **2013**, *135*, 2338−2349.
(73) Street, R. A.; Northrup, J. E.; Salleo, A. *Phys. Rev. B* **2005**, *71*, 165202.
(74) Kline, R. J.; DeLongchamp, D. M.; Fischer, D. A.; Lin, E. K.; Heeney, M.; McCulloch, I.; Toney, M. F. *Appl. Phys. Lett.* **2007**, *90*, 062117.
(75) Huang, H.; Chen, Z.; Ortiz, R. P.; Newman, C.; Usta, H.; Lou, S.; Youn, J.; Noh, Y.-Y.; Baeg, K.-J.; Chen, L. X.; Facchetti, A.; Marks, T. *J. Am. Chem. Soc.* **2012**, *134*, 10966−10973.